iCharge: User-Interactive Charging of Mobile Devices

Liang He
University of Michigan
2260 Hayward St.
Ann Arbor, MI, 48109
lianghe@umich.edu

Yu-Chih Tung
University of Michigan
2260 Hayward St.
Ann Arbor, MI, 48109
yctung@umich.edu

Kang G. Shin
University of Michigan
2260 Hayward St.
Ann Arbor, MI, 48109
kgshin@umich.edu

ABSTRACT

Charging mobile devices "fast" has been the focus of both industry and academia, leading to the deployment of various fast charging technologies. However, existing fast charging solutions are agnostic of users' available time for charging their devices, causing early termination of the intended/-planned charging. This, in turn, accelerates the capacity fading of device battery and thus shortens the device operation. In this paper, we propose a novel user-interactive charging paradigm, called `iCharge`, that tailors the device charging to the user's real-time availability and need. The core of `iCharge` is a relaxation-aware (`R-Aware`) charging algorithm that maximizes the charged capacity within the user's available time and slows down the battery's capacity fading. `iCharge` also integrates `R-Aware` with existing fast charging algorithms via a user-interactive interface, allowing users to choose a charging method based on their availability and need. We evaluate `iCharge` via extensive laboratory experiments and field-tests on Android phones, as well as user studies. `R-Aware` is shown to slow down the battery fading by more than 36% on average, and up to 60% in extreme cases, when compared to existing fast charging algorithms. This slowdown of capacity fading translates to, for instance, an up to 2-hour extension of the LTE time for a Nexus 5X phone after its use for 2 years, according to our trace-driven analysis of 976 device charging cases of 7 users over 3 months.

Keywords

Mobile devices; battery fading; user-interactive charging; battery relaxation

1. INTRODUCTION

The limited operation time of mobile devices, such as smartphones, tablets, and laptops, has become the main gripe of user experience, especially with their increasing functionalities and computation demands [6, 28]. Moreover, batteries become weaker with usage, known as *capacity fading* [26, 34, 38, 46], shortening the device operation time [14]. For example, an over 50% capacity fading of a 14-month-old Galaxy S4 battery was reported [12]; our measurements with a Galaxy S6 Edge phone show a 14% battery capacity fading over 4 months of real-life usage.[1] Also, our user study with 146 participants shows that 89% of them noticed their device operation time shortened under normal usage patterns and 70% of them view it as crucial.

Charging mobile devices "fast" alleviates the users' concern on the limited device operation time by replenishing the devices with energy faster. This has been the focus of both industry and academia, developing and deploying various fast charging technologies, such as Quick Charge 3.0 by Qualcomm [5], TurboPower by Motorola [10], VOOC Flash Charge by OPPO [11], to name a few.

Fast charging, unfortunately, accelerates the capacity fading of device battery owing to, besides the high charging rate [14], the joint effects of two properties they share: the basic principle of *Constant Current, Constant Voltage* (CCCV) charge and *user-agnosia*. State-of-the-art fast charging technologies, in general, follow the classical CCCV charging for Li-ion batteries [12, 42] — a two-phase charging process consisting of (i) Constant-Current Charge (CC-Chg) and (ii) Constant-Voltage Charge (CV-Chg). Also, these fast charging technologies are agnostic of users' time availability for charging their devices. Implicitly assuming the availability of sufficient charging time, they blindly try to fully charge the devices, resulting in premature termination of the planned charging if users only have limited time. This, in turn, leads to an incomplete or even skipping the CV-Chg phase. Our empirical measurements, however, reveal that *CV-Chg relaxes the batteries and slows down their capacity fading by up to* 80% — an incomplete CV-Chg shortens the battery life faster!

This limitation of fast charging motivated us to design `iCharge`, a novel user-interactive charging paradigm that tailors the device charging to the users' availability and need.[2] At the core of `iCharge` is a relaxation-aware (`R-Aware`) charging algorithm that plans the device charging based on the users' available time. `R-Aware` maximizes the charged capacity while ensuring the use of CV-Chg to relax the battery, thus improving battery health and device

MobiSys'17, June 19-23, 2017, Niagara Falls, NY, USA

DOI: http://dx.doi.org/10.1145/3081333.3081350

[1] The capacity fading rate depends on the device-usage pattern.

[2] `iCharge` applies to any battery-powered systems, including electric vehicles where the batteries are a significant portion of their weight and cost.

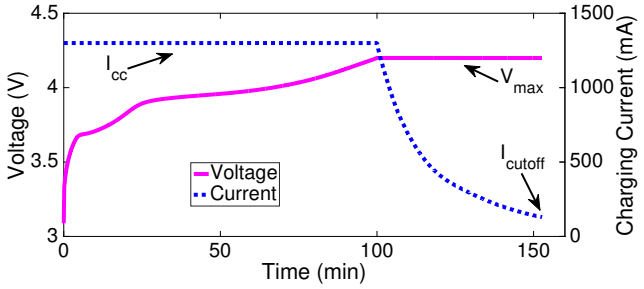

Figure 1: CCCV-based charging process: the battery is first charged with CC-Chg and then CV-Chg.

operation time in the long run. Note that CV-Chg is slow in charging the device, thus limiting the power of charging devices. To remedy this problem, `R-Aware` shortens and triggers the CV-Chg phase earlier than the original CCCV by introducing a new control knob to CCCV and determining the proper charging profiles based on the user's available time. We have evaluated `R-Aware` via laboratory experiments over 15 months with advanced battery testing systems, discovering a more than 36% slowdown of battery capacity fading. These experimental results, coupled with real-life user traces of more than 20 months, show `R-Aware` extends the LTE time of a Nexus 5X phone by up to 2 hours over 2 years.[3] We have also implemented `R-Aware` as a system component on various Android devices, corroborating its compatibility with commodity devices.

`R-Aware` offers an attractive alternative to keep the device battery healthier at the expense of a slower charging rate. To preserve user experience when a high charging rate is required, `iCharge` also integrates/combines `R-Aware` with fast charging via easy-to-use interactions between users and the charger. Specifically, `iCharge` allows the users to specify their available charging time, displays the charged capacity if `R-Aware` or fast charging is used, and adopts the user's selection of a charging method in the charging plan.

This paper makes the following contributions:

- Discovery and demonstration of CV-Chg's slowdown of battery capacity fading, and absence of its use in state-of-the-art charging of mobile devices (Sec. 2);
- Development of a novel charging paradigm for mobile devices, `iCharge`, that slows down their battery fading with a novel charging algorithm, `R-Aware`, and allows the users to interactively choose a method for tailoring their device charging to their availability and need (Sec. 3);
- Extensive evaluation of `iCharge` via laboratory experiments (Sec. 4), implementation on commodity Android phones (Sec. 5), and user-studies (Sec. 6).

The paper is organized as follows. Sec. 2 motivates the design of `iCharge`, while Sec. 3 provides its details. `iCharge` is evaluated extensively in Secs. 4–6. Further issues relevant to `iCharge` are discussed in Sec. 7. Sec. 8 reviews the related literature, and the paper concludes in Sec. 9.

[3]A new Nexus 5X is reported to have an 8-hour LTE time [3].

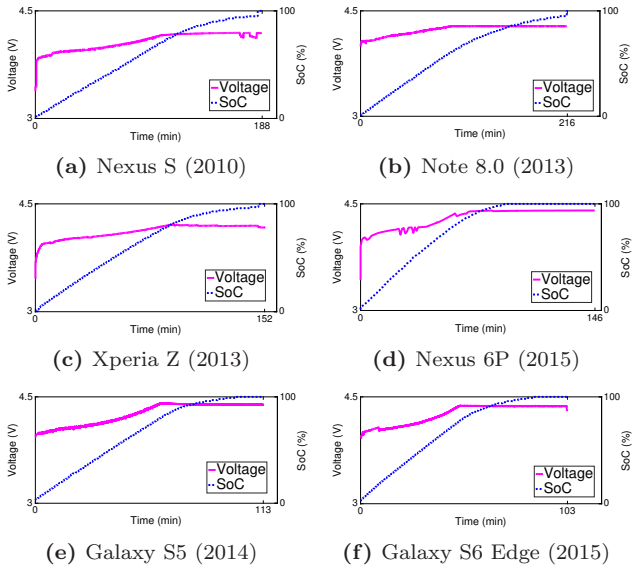

Figure 2: Charging mobile devices with respective chargers, showing (i) shortened charging time with the advancement of charging technologies, (ii) CCCV charging in principle, and (iii) CV-Chg takes long and is slow in charging.

2. CHARGING AFFECTS FADING

Batteries get weakened over usage, shortening their device operation time [8]. For example, an over 50% capacity fading of a 14-month-old Galaxy S4 battery is reported in [12], shortening device operation time by over 4 hours. The capacity fading of device batteries becomes more critical as mobile devices with non-replaceable batteries — such as iPhones and Galaxy S6 and their descendants — are becoming a new trend.

The capacity fading of batteries is inevitable due to their intrinsic electrochemical characteristics, e.g., loss of active materials over usage [26,34,38,46]. Their fading rates, however, depend on their usage pattern. In this paper, we focus on how the charging of mobile devices affects the fading of their battery capacity.

2.1 Fast Charging

Various fast charging technologies have been developed and deployed to improve user experience. These technologies can be viewed as various extensions of the classical two-phase CCCV charging of Li-ion batteries, described by

$$< I_{\rm cc},\ V_{\rm max},\ I_{\rm cutoff} >_{\rm cccv} . \qquad (1)$$

First, the battery is charged with a large and constant current $I_{\rm cc}$ (normally 0.5–1C) until its voltage reaches the fully-charged level $V_{\rm max}$ (e.g., 4.25V), i.e., Constant-Current Charge (CC-Chg), during which its state-of-charge (SoC) increases quickly.[4] Then, the battery is charged further by a constant voltage $V_{\rm max}$ until the charging current decreases to a pre-defined cutoff level $I_{\rm cutoff}$ (normally 0.025–0.05C), fully charging the battery. This second phase is called the *Constant-Voltage Charge* (CV-Chg). Fig. 1 plots our empirically collected data of CCCV-based charging of a Li-ion battery.

[4]The charging (and discharging) currents of batteries are often expressed in *C-rate*. For example, in case of discharging, a 1 C-rate means that the current drains the battery completely in 1 hour, i.e., 3,100mA for 3,100mAh batteries.

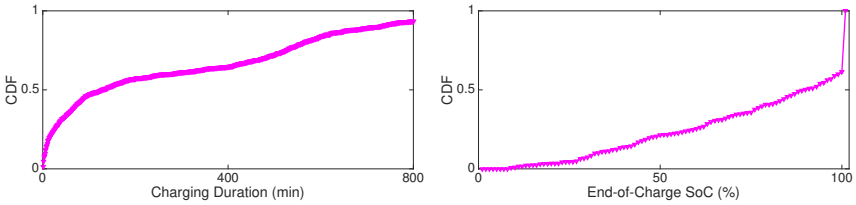

(a) Charging duration **(b)** End-of-Charge SoC

Figure 3: Users' charging behavior (only the first 800 minutes of the charging process are shown for clarity): device charging is likely to be prematurely terminated.

Figure 4: Experiment bench.

Table 1: Statistics of users' charging behavior.

User	#1	#2	#3	#4	#5	#6	#7
Incomp. Ratio	0.93	0.69	0.60	0.51	0.63	0.14	0.80
# Charges / Day	2.05	2.41	1.40	2.28	1.57	1.76	3.79

To examine how this CCCV principle is implemented in commodity devices, we record the charging processes of 6 mobile devices as shown in Fig. 2 — from depleted to fully charged and with their respective chargers — and make the following three key observations.

1. The time to fully charge these devices has been shortened with the advancement of charging technologies, e.g., from 188 minutes for Nexus S released in 2010 to 113 minutes for the 2014 Galaxy S5, but it still takes about 100 minutes to fully charge even for the fastest charging Galaxy S6 Edge.
2. All of these charging processes, in principle, follow the CCCV charging — the devices are charged quickly during the first phase until their batteries reach about 4.25–4.4V, after which a constant voltage is applied until they become fully charged.
3. CC-Chg is the major phase to charge devices. In contrast, CV-Chg is slow and takes long in charging the device batteries, e.g., CV-Chg for Galaxy S6 Edge takes ≈55% of the total time to charge the last 20% capacity.

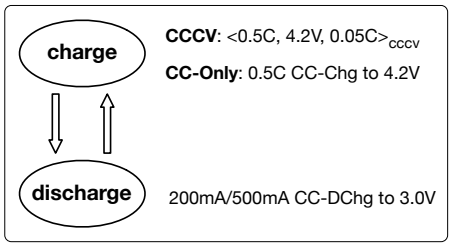

Figure 5: Cycling test methodology.

2.2 Users' Charging Behavior

To see how these charging technologies are used in real-life, we plot in Fig. 3(a) the charging time distributions of 976 cases collected from 7 users over 3 months.[5] About

[5]One of the user-traces was collected from our data-collection campaign and the other six traces were obtained from the sample dataset of Device Analyzer from Cambridge University [44].

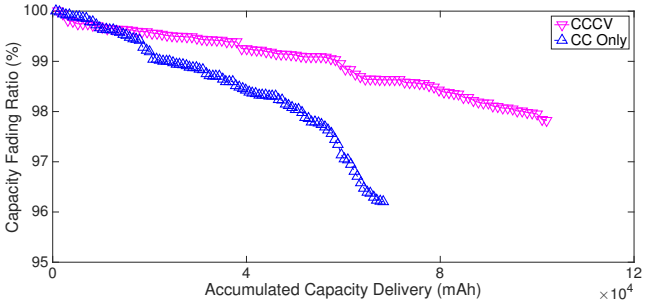

Figure 6: Capacity fading of the Nexus S battery over 100 cycles.

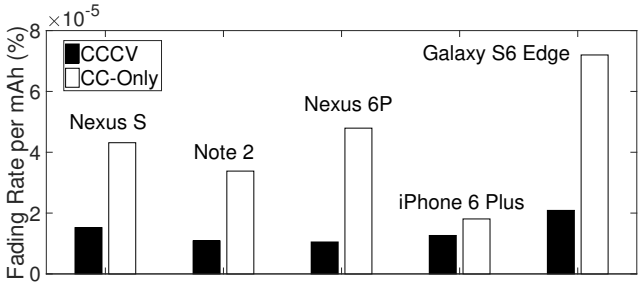

Figure 7: Capacity fading of 5 phone batteries over 100 cycles, showing the slow-down of capacity fading with CV-Chg.

50% of the charging is observed to last less than 2 hours, representing the device charging during daytime [24]. Comparison of this with Fig. 2 indicates that these short charging durations may not be enough to fully charge the devices. To validate this, we record the battery SoC (State-of-Charge) — an indicator of battery's remaining capacity in percentage (0% = empty; 100% = full) — when the charging is terminated, and plot their distributions in Fig. 3(b). As expected, the device charging is prematurely terminated, leading to an incomplete CV-Chg with a 61% probability. Table 1 shows the details of the individual users' charging behavior. Moreover, 80% SoC is considered as the threshold for the charging to switch from CC-Chg to CV-Chg, which is roughly the case shown in Fig. 2. This way, we find about 41% of charging cases terminated prematurely without CV-Chg at all.

2.3 CV-Chg Slows Down Capacity Fading

Skipping the slow and long CV-Chg does not reduce the charged capacity much. However, *CV-Chg slows down the capacity fading of batteries and thus improves their lifetime* — a new discovery from our measurement study.

We conducted cycling tests with the batteries of Nexus S, Note 2, Nexus 6P, iPhone 6 Plus, and Galaxy S6 Edge to corroborate this finding. The 8-channel NEWARE battery testers are used as both the charger and the load, with which the battery charging and discharging can be programmed with error $\leq$0.05% and logged at frequency up to 10Hz. Fig. 4 shows our lab bench for these experiments. We charge and discharge the batteries 100 times/cycles with completed CCCV (i.e., ensuring the use of CV-Chg) and CC-Chg only (i.e., skipping CV-Chg), respectively, as illustrated in Fig. 5. We record the batteries' capacity delivery during each discharging to calculate their capacity fading ratio — the ratio of the delivered capacity during the i-th cycle to that during the first cycle. Fig. 6 illustrates the degradation of the Nexus S battery during the measurement. Fig. 7 plots the batteries' fading ratios after these cycling tests, showing that CV-Chg reduces battery fading by 0.00003% per-delivered-capacity — an averaged slowdown of 62.35% and up to 80% in some extreme cases, e.g., for the Nexus 6P battery.

2.4 Why Does CV-Chg Help?

Li-ion batteries operate according to the principle of intercalation: during charging, Li-ions is extracted from the lattice of the active materials at the cathode, and then inserted at the anode; the process is reversed for discharging. The insertion of Li-ions causes volume expansion of the materials' lattice structure, while extraction causes contraction. The expansion and contraction are pronounced with large currents and their frequency depends on the switching between charging and discharging. High magnitude and frequency of expansion/contraction accelerate the fracture of lattice structure, leading to permanent loss of active materials and thus capacity fading of Li-ion batteries [2, 34]. Gradually decreasing CV-Chg current allows the anode's (cathode's) lattice volume to equilibrate after the intensive expansion (contraction) caused by CC-Chg and before its contraction (expansion) during the following discharging, relaxing the active materials. This slows down the fracture of lattice structure and thus battery fading. The decreasing current also reduces battery heating, another key contributor to battery degradation.

Note that both the insertion and extraction of Li-ions are achieved via chemical reactions requiring certain time, which could fail if the current is terminated before their completion. For battery charging, this is reflected by a battery voltage drop upon the current termination, a key consideration in our design (Sec. 3.3).

3. USER-INTERACTIVE CHARGING

The user-agnosia of existing charging solutions motivated us to design `iCharge`, which integrates existing fast charging with a novel relaxation-aware (`R-Aware`) charging algorithm via user interactions, providing users customized device charging.

Fig. 8 presents an overview of `iCharge`. Upon connection of the charger, a user interface — consisting of a seekbar and two buttons — prompts. The seekbar allows the user to specify his available time for device charging and the buttons show the charging results with `R-Aware` and fast charging, respectively. The user chooses his preferred charging profile — how long to charge with which method — based on his availability and need simply by clicking the corresponding button, and then the device will be charged accordingly.

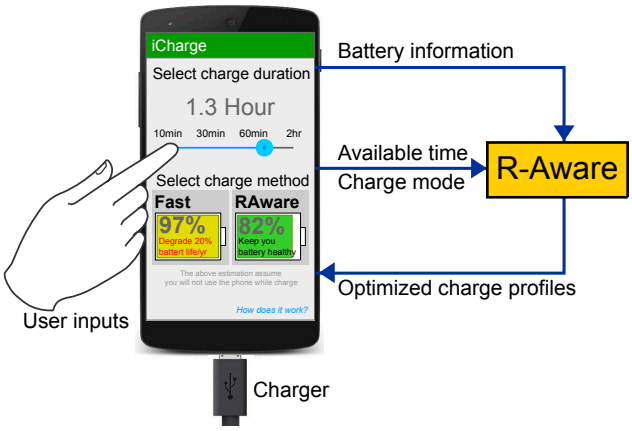

Figure 8: `iCharge` overview: tailoring the device charging to the user's available time and selection of charging method.

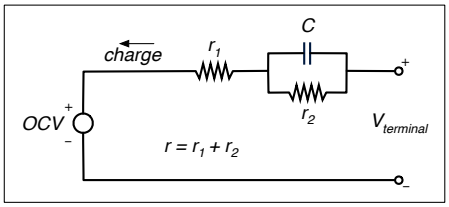

Figure 9: Battery circuit model.

3.1 Background

To facilitate the understanding of `iCharge`, we first introduce the necessary background on battery charging.

3.1.1 *Open-Circuit and Terminal Voltages*

Battery voltage plays a key in its charging. The open-circuit voltage (OCV) of a battery is the voltage between its terminals without connecting load, which becomes the terminal voltage of the battery when load is connected. In other words, OCV is an inherent battery property and the terminal voltage is what is measured in practice. Fig. 9 shows the commonly used battery circuit model, from which we get

$$V_{\text{terminal}} = OCV + I \cdot (r_1 + r_2), \tag{2}$$

where I is the current charging the battery, and r_1 and r_2 are the battery's ohmic and capacitive resistance, respectively. We use the term "voltage" for convenience to mean the terminal voltage, and define $r = r_1 + r_2$.

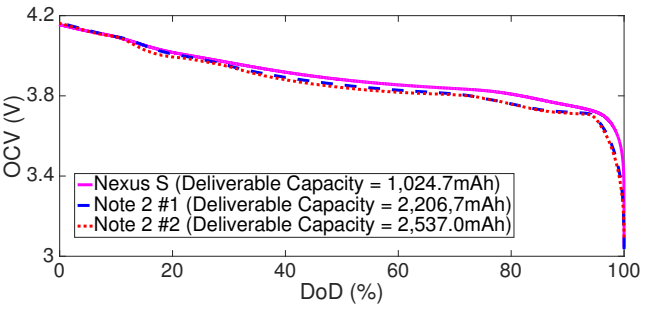

Figure 10: Non-linearity between battery OCV and DoD.

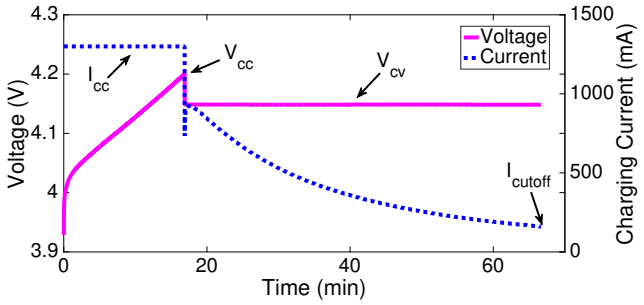

Figure 11: `R-Aware`-based charging process.

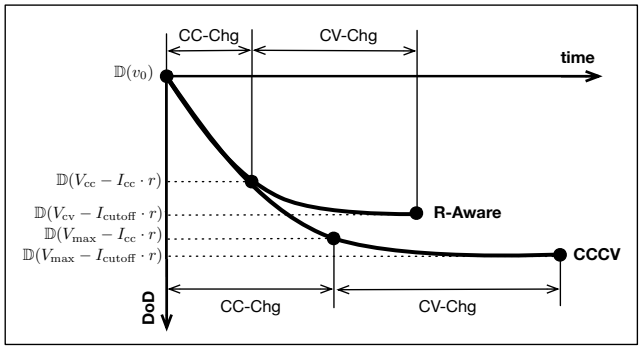

Figure 12: Comparison between `R-Aware` and CCCV: `R-Aware` initiates CV-Chg earlier and makes it shorter.

3.1.2 Non-Linearity between OCV and DoD

Batteries exhibit a monotonic relationship between their OCVs and DoDs (Depth-of-Discharge).[6] This relation is stable for batteries of the same chemistry and does not vary much with manufacturers (e.g., <5mV variances in OCV with given DoD [1]). Fig. 10 plots our empirically collected OCV–DoD curves with one Nexus S battery and two Note 2 batteries. Although these batteries are different in both rated and deliverable capacities, their OCV–DoD curves are close to each other, thus validating the stable OCV–DoD relation. We will in Sec. 4.1 elaborate on how the curves in Fig. 10 are obtained. This monotonic OCV–DoD relation allows the mapping between them, denoted as $\mathbb{D}(v)$ and $\mathbb{O}(d)$, respectively, in the rest of the paper.

Fig. 10 also shows that the OCV–DoD relation is not linear — the OCVs are more sensitive to DoDs when the batteries are nearly fully charged (e.g., below 20% DoD) or completely discharged (e.g., approaching 100% DoD), but are not very sensitive in certain middle ranges, e.g., between 40–80% DoD. This non-linearity plays a crucial role in battery charging, as we shall see later.

3.2 Design Overview

As the core of `iCharge`, `R-Aware` offers an alternative to fast charging when fast charging is not strictly required. `R-Aware` takes the user's available time and other battery information such as its OCV–DoD table and initial OCV v_0 as input, and then plans the charging process to maximize the charged capacity while ensuring the use of CV-Chg.

[6]DoD describes the battery capacity that has been discharged as the percentage of its maximum capacity, i.e., the inverse of SoC (100% = empty; 0% = full).

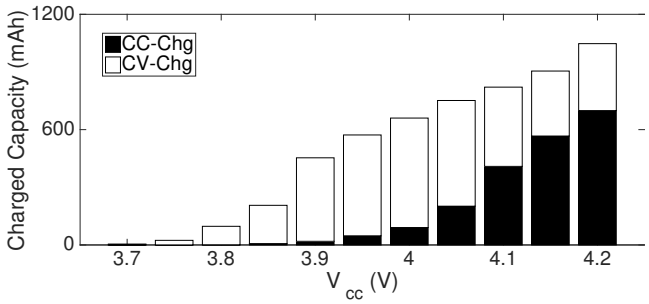

(a) V_{cc} w.r.t. charged capacity

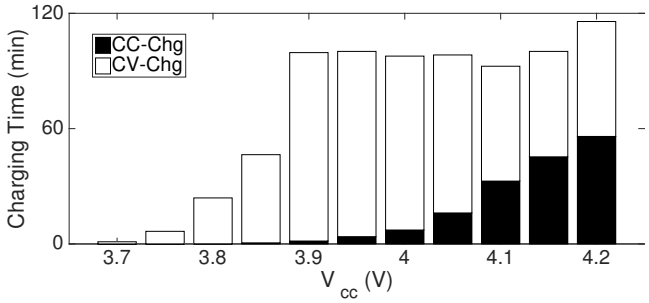

(b) V_{cc} w.r.t. charging time

Figure 13: A smaller V_{cc} leads to less charged capacity but not necessarily shorter charging time.

`R-Aware` is also an extended CCCV, i.e., a two-phase charging algorithm described by four control knobs

$$< I_{cc}, V_{cc}, V_{cv}, I_{cutoff} >_{\texttt{R-Aware}} \quad (V_{cv} \le V_{cc} \le V_{max}). \quad (3)$$

The `R-Aware`-based charging process starts with CC-Chg with current I_{cc} until the battery voltage rises to V_{cc}, and then the battery is charged with CV-Chg with voltage V_{cv} until the current falls to I_{cutoff}, as illustrated in Fig. 11. This way, the key to `R-Aware` is identifying a proper combination of the four control knobs in (3).

3.2.1 Earlier and Shorter CV-Chg by R-Aware

CV-Chg takes long and is slow in charging rate, hence limiting the charged capacity within the available time. `R-Aware` remedies this problem by initiating it earlier and making it shorter. This is illustrated in Fig. 12 which shows the battery's DoD trace during the `R-Aware`-based charging process and compares it with that of the original CCCV.

`R-Aware` first extends CCCV by reducing V_{max} to V_{cc}. This way, CC-Chg charges the battery to the OCV of $V_{cc} - I_{cc} \cdot r$, which is smaller than the original CCCV (i.e., $V_{max} - I_{cc} \cdot r$), leading to shorter CC-Chg and thus triggering CV-Chg earlier.

Triggering CV-Chg earlier alone, however, may lead to a longer CV-Chg. This also leads to an interesting finding that, when the use of a complete CV-Chg is required, charging less capacity does not necessarily result in a shorter charging time.

To demonstrate this, we use the profiles of $<0.5C, V_{cc}, 0.05C>_{cccv}$ to charge a Nexus S battery with various V_{cc} from 3.7V to 4.2V. Fig. 13 compares the charged capacity and the charging durations, showing that a smaller V_{cc} leads to less charged capacity but not necessarily a shorter charging time. This discrepancy between charged capacity and charging time is due to the nonlinearity between the

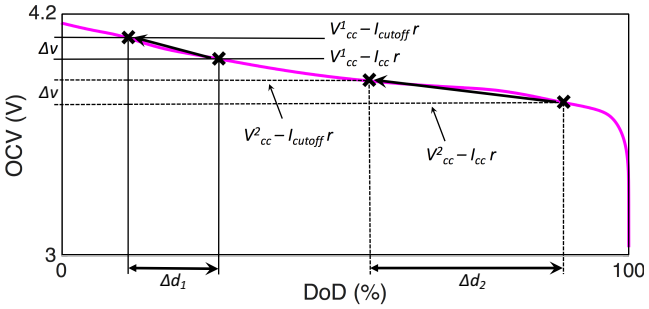

Figure 14: Same magnitude of OCV change may lead to significantly different magnitudes of DoD changes.

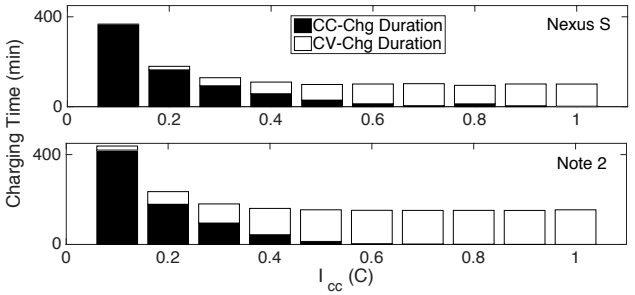

Figure 15: Over-large I_{cc} cannot further shorten the charging process.

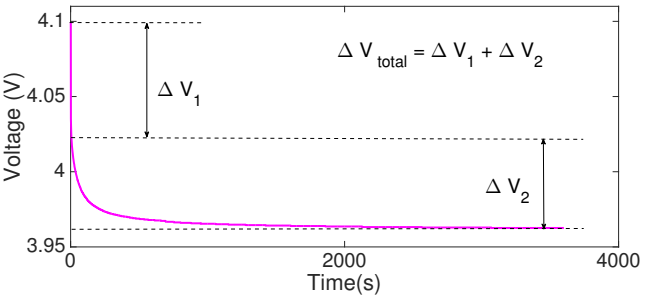

Figure 16: Two-phase voltage drop after terminating the charging current.

battery's OCV and DoD. Let's consider the case when reducing V_{cc} from V_{cc}^1 to V_{cc}^2 ($V_{\text{cc}}^1 > V_{\text{cc}}^2$). From Fig. 12, we know the OCV range within which CC-Chg applies shrinks from $[v_0,\ \ V_{\text{cc}}^1 - I_{\text{cc}} \cdot r]$ to $[v_0,\ \ V_{\text{cc}}^2 - I_{\text{cc}} \cdot r]$, leading to shorter CC-Chg. However, the OCV ranges for which CV-Chg is responsible are $[V_{\text{cc}}^1 - I_{\text{cc}} \cdot r,\ \ V_{\text{cc}}^1 - I_{\text{cutoff}} \cdot r]$ and $[V_{\text{cc}}^2 - I_{\text{cc}} \cdot r,\ \ V_{\text{cc}}^2 - I_{\text{cutoff}} \cdot r]$ before and after the change, respectively. These OCV ranges may map to different DoD intervals (and thus to-be-charged capacities) because of the nonlinear OCV–DoD table, albeit sharing the same OCV gap of $(I_{\text{cc}} - I_{\text{cutoff}}) \cdot r$. Fig. 14 illustrates the case in which the same magnitude of OCV change (i.e., Δv) results in significantly different magnitudes of DoD changes (i.e., $\Delta d_1 << \Delta d_2$). Thus, a smaller V_{cc} shortens CC-Chg, but may lead to longer CV-Chg — the overall charging time is not necessarily reduced.

`R-Aware` further extends CCCV by providing another control knob $V_{\text{cv}} (V_{\text{cv}} \leq V_{\text{cc}})$ to reduce the OCV range of CV-Chg from $[V_{\text{cc}} - I_{\text{cc}} \cdot r,\ \ V_{\text{cc}} - I_{\text{cutoff}} \cdot r]$ to $[V_{\text{cc}} - I_{\text{cc}} \cdot r,\ \ V_{\text{cv}} - I_{\text{cutoff}} \cdot r]$, making CV-Chg shorter.

3.2.2 *Algorithm Overview*

Alg. 1 provides an overview of `R-Aware`, which will be detailed later. `R-Aware` adopts I_{cc} as in the fast charging implementation of the corresponding device (line 1), and then identifies I_{cutoff} that offers sufficient relaxation to the battery (line 2–3). The two control knobs on voltages are identified by searching down the potential voltage range with a granularity of δ_v (line 4–9). `R-Aware` has a complexity of $\mathcal{O}(log(\frac{V_{\max} - v_0}{\delta_v}))$ when using binary search in the **for** loop.

Algorithm 1 `R-Aware` Charging.

1: set I_{cc} as in fast charging;
2: estimate r_1 and r_2 by (4) and (6);
3: determine I_{cutoff} by (5);
4: **for** $V_{\text{cc}} = V_{\max} : -\delta_v : v_0$ **do**
5: $\quad V_{\text{cv}} = V_{\text{cc}} - I_{\text{cc}} \cdot r_1$ (as in (7));
6: $\quad$ estimate C_{total}, C_{cc} and C_{cv} by (8), (9), and (11);
7: $\quad$ estimate T_{cc} and T_{cv} by (10) and (13);
8: $\quad$ **if** $T_{\text{cc}} + T_{\text{cv}} \leq T_{\text{available}}$ **then**
9: $\quad\quad$ **break;**
10: $\quad$ **end if**
11: **end for**
12: **return** $<I_{\text{cc}}, V_{\text{cc}}, V_{\text{cv}}, I_{\text{cutoff}}>_{\texttt{R-Aware}}$;

3.3 Design Details

We now discuss how to determine the four control knobs in `R-Aware`.

3.3.1 *Identifying* I_{cc}

Intuitively, a larger I_{cc} shortens the charging process. An over-large current, however, has a diminishing effect on further reduction of the charging time, as shown in Fig. 15 where Nexus S and Note 2 batteries are charged with I_{cc} that varies from 0.1C to 1.0C. This is because CC-Chg charges the battery to $(V_{\text{cc}} - I_{\text{cc}} \cdot r)$, and CV-Chg further charges it to $(V_{\text{cv}} - I_{\text{cutoff}} \cdot r)$. All things being equal, a larger I_{cc} completes CC-Chg faster but extends the OCV range of CV-Chg. Whether or not the overall charging process is shortened is unclear.

Also, a larger charging current leads to a faster temperature rise of the battery, due to the heating of its internal resistance. The charging current has to be reduced to cool the battery once its temperature rises to a pre-defined safety threshold [39], e.g., 45°C for Nexus 5X. This, again, indicates that a larger I_{cc} may not always be good.

As a result, instead of employing larger charging currents, `R-Aware` uses the same I_{cc} as in the fast charging implementation of the corresponding device.

3.3.2 *Identifying* I_{cutoff}

CV-Chg slows down the battery fading by allowing it to equilibrate, but is slow in charging the battery. `R-Aware` ensures a CV-Chg to be only long enough for equilibration, which is, in turn, indicated by the battery's voltage-drop after terminating the charging current. Fig. 16 plots the battery voltage during a 1-hour idle period after terminating the charging current. The voltage drops instantly by a certain level (i.e., ΔV_1) upon current termination, then it decreases gradually by another level (i.e., ΔV_2). This can be explained with the battery circuit model in Fig. 9 — the instantaneous drop ΔV_1 is due to the immediate disappearance of voltage across r_1 upon current termination, and the

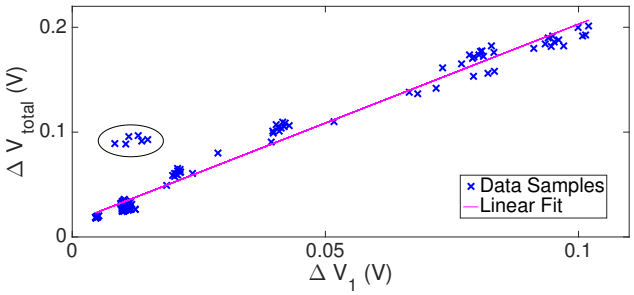

Figure 17: Linearity between instant voltage drop (ΔV_1) and total drop (ΔV_{total}).

Table 2: Measurement settings to validate $\Delta V_{\text{total}} = a \cdot \Delta V_1 + b$.

# Batt.	Ini. V.	I_{cc}	V_{cc}	V_{cv}	I_{cutoff}
7	3.0–3.24V	0.19–1C	3.8–4.2V	3.8–4.2V	0.025–0.4C

following gradual drop ΔV_2 is due to the gradual effect of r_2, thanks to the parallel capacitor. Fuller *et al.* [25] have shown that ΔV_2 is the result of relaxation and a smaller V_2 indicates a closer equilibrium. This way, `R-Aware` uses I_{cutoff} that ensures small enough ΔV_2, e.g., 0.02V.

We estimate ΔV_2 with given I_{cutoff} based on an empirical finding that ΔV_1 is linear in $\Delta V_{\text{total}} = \Delta V_1 + \Delta V_2$, i.e., $\Delta V_{\text{total}} = a \cdot \Delta V_1 + b$ for certain coefficients a and b, and thus linear in ΔV_2 as well. Fig. 17 shows such a plot based on 152 voltage-drop traces after charging batteries with profiles summarized in Table 2. Most of these data samples follow a linear relation well, e.g., the linear fit shown in Fig. 17 has a mean-squared error of 1.77e-04. Outliers, however, exist as highlighted. A closer examination reveals a common feature in them that there is no CV-Chg in their corresponding charging traces. This linear relation allows us to estimate ΔV_2 if we can (i) identify the linear coefficients, (ii) estimate ΔV_1, and (iii) ensure CV-Chg is used during charging.

`R-Aware` learns these linear coefficients by collecting the voltage-drop traces of idle batteries from a device-charging history, and linear fitting ΔV_1s and ΔV_{total}s therein. This is feasible because of the separated power paths of mobile devices as shown in Fig. 18 [16]. The charger power is separated into two flows to power the device and charge the battery, allowing the battery to rest and thus collecting its voltage-drop traces, e.g., by keeping the charger connected after fully charging the battery during night-time. To verify this, we kept the charger connected after fully charging a Nexus 6P phone and recorded its battery voltage and current, as shown in Fig. 19. The battery current reduces to, and stays at 0mA after the charging is completed, and its voltage drops first instantly and then gradually, agreeing with Fig. 16.[7]

Next let's consider the estimation of ΔV_1. According to the basic physics, $\Delta V_1 = I_{\text{cutoff}} \cdot r_1$ for any charging process ending with I_{cutoff}, so the question transforms to the estimation of r_1 after the charging completion. `R-Aware` estimates r_1 by applying a current pulse I to the battery before charging it, and monitoring its instant voltage response Δv, i.e.,

$$r_1 = \frac{\Delta v}{I}. \tag{4}$$

However, this before-charge r_1 may differ from the after-charge r_1, because battery resistance varies over time [32]. Again, we show via measurements that r_1 does not vary much over a single charge of batteries. Fig. 20 compares r_1 measured before and after charging the batteries based on 115 empirically collected traces. The fact that most samples fall along the line of $y = x$ supports `R-Aware` to use the before-charge r_1 to estimate that after charging. This way, we can compute ΔV_1 via $\Delta V_1 = I_{\text{cutoff}} \cdot r_1$, and thus $\Delta V_{\text{total}} = a \cdot (I_{\text{cutoff}} \cdot r_1) + b$. `R-Aware` determines the desired I_{cutoff} as

$$\Delta V_2 \le \theta \quad \Leftrightarrow \quad I_{\text{cutoff}} \le \frac{\theta - b}{(a-1) \cdot r_1}. \tag{5}$$

We can also estimate r_2 by

$$r_2 = \frac{\Delta V_{\text{total}} - \Delta V_1}{I_{\text{cutoff}}}. \tag{6}$$

Knowing how to determine the proper I_{cutoff} when CV-Chg is used during charging, we must now explore how to ensure its usage by identifying a proper V_{cv}.

3.3.3 *Identifying* V_{cv}

A voltage higher than the battery voltage is required to charge it, i.e., V_{cv} must be higher than the battery voltage when switching from CC-Chg to CV-Chg. From the circuit model in Fig. 9, we know the battery voltage would drop to $(V_{\text{cc}} - I_{\text{cc}} \cdot r_1)$ instantly when CC-Chg is terminated without starting CV-Chg, such that

$$V_{\text{cv}} \ge V_{\text{cc}} - I_{\text{cc}} \cdot r_1.$$

On the other hand, Fig. 12 shows that a larger V_{cv} extends the OCV range for charging the battery with CV-Chg, indicating that a small V_{cv} is desired to shorten the CV-Chg period. The combination of these two observations makes `R-Aware` set V_{cv} as

$$V_{\text{cv}} = V_{\text{cc}} - I_{\text{cc}} \cdot r_1. \tag{7}$$

3.3.4 *Identifying* V_{cc}

The last step is to identify V_{cc}, which, together with the above-identified control knobs, maximizes the charged capacity within the user's available time $T_{\text{available}}$. The total charged capacity with `R-Aware` is

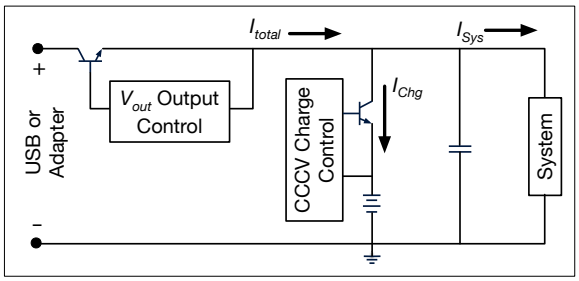

Figure 18: Separate power paths from the charger to the battery and the system, allowing the battery to rest after being fully charged [16].

[7]Certain mobile devices use trickle charging to keep their batteries fully charged after reaching 100% SoC, which prevents batteries to stay resting. Relaxing sub-traces, however, can still be observed and collected.

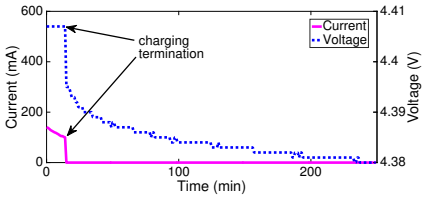

Figure 19: Resting a Nexus 6P battery after fully charging it.

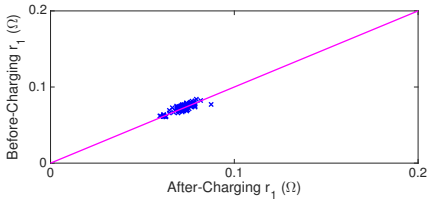

Figure 20: The ohmic resistance r_1 is stable before and after charging.

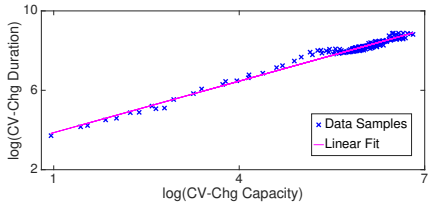

Figure 21: Log-log plot of T_{cv} and C_{cv} demonstrates a linear relation.

Table 3: Measurement settings to validate $log(T_{\text{cv}}) = c \cdot log(C_{\text{cv}}) + d$.

# Batt.	Ini. OCV	I_{cc}	V_{cc}	V_{cv}	I_{cutoff}
4	3.36–3.74V	0.5–1C	3.90–4.20V	3.89–4.19V	0.05–0.1C

Table 4: Collected charging traces to validate `R-Aware`'s accuracy.

# of Batt.	Ini. OCV	I_{cc}	V_{cc}	V_{cv}	I_{cutoff}
8 × 2,600mAh	3.37 – 3.81V	0.5 – 1C	3.9 – 4.2V	3.85 – 4.2V	0.05 – 0.1C

Table 5: Experimental settings.

Cases	Ava. Time	Ini. OCV	θ
I	100min	3.120V	0.02V
II	90min	3.232V	0.02V
III	70min	3.866	0.02V
IV	70min	3.853	0.02V
V	60min	3.200V	0.02V
VI	60min	3.878V	0.02V
VII	55min	3.869V	0.02V
VIII	30min	3.505V	0.02V

$$C_{\text{total}} = \frac{C_0 \cdot (\mathbb{D}(v_0) - \mathbb{D}(V_{\text{cv}} - I_{\text{cutoff}} \cdot r))}{100} = \frac{C_0 \cdot (\mathbb{D}(v_0) - \mathbb{D}(V_{\text{cc}} - I_{\text{cc}} \cdot r_1 - I_{\text{cutoff}} \cdot r))}{100} \quad (8)$$

where C_0 is the total battery capacity when it is fully charged, e.g., 1024.7mAh for the Nexus S battery as shown in Fig. 10.

All things being equal, a larger V_{cc} leads to a larger C_{total} since $\mathbb{D}(v)$ monotonically decreases with v. So, we search down the potential ranges of V_{cc} and return the first charging profile that completes within $T_{\text{available}}$, which charges the device to the maximum capacity. This, however, requires estimation of the charging duration with a given `R-Aware`-based charging profile: the CC-Chg duration T_{cc} and the CV-Chg duration T_{cv}.

The charged capacity and the charging time of `R-Aware`-based CC-Chg can be computed by

$$C_{\text{cc}} = \frac{C_0(\mathbb{D}(v_0) - \mathbb{D}(V_{\text{cc}} - I_{\text{cc}} \cdot r))}{100} \quad (9)$$

$$T_{\text{cc}} = \frac{C_{\text{cc}}}{I_{\text{cc}}}. \quad (10)$$

So, we can estimate C_{cv} based on (8) and (9) by

$$C_{\text{cv}} = C_{\text{total}} - C_{\text{cc}}. \quad (11)$$

Moreover, our measurements show T_{cv} and C_{cv} to be log-log-linear to each other, i.e., $log(T_{\text{cv}}) = c \cdot log(C_{\text{cv}}) + d$, based on which T_{cv} can be estimated. To demonstrate this, Fig. 21 shows the log-log plot of T_{cv} and C_{cv} from 174 charging traces, along with their corresponding linear fit $log(T_{\text{cv}}) = 0.8648 \cdot log(C_{\text{cv}}) + 3.0024$, which has a mean-squared error of 0.0162. The details of these traces are summarized in Table 3. The log-log-linearity holds because the current trace of CV-Chg conforms to the shape of $I_{\text{cv}}(t) = A \cdot t^B$, as illustrated in Fig. 11. This way, we know

$$C_{\text{cv}} = \int_0^{T_{\text{cv}}} I_{\text{cv}}(t)dt = \frac{A}{B+1} T_{\text{cv}}^{B+1}, \quad (12)$$

and thus $\log(T_{\text{cv}}) = \frac{1}{B+1}\log(C_{\text{cv}}) - \frac{1}{B+1}\log(\frac{B+1}{A})$, demonstrating a log-log-linear relation. Again, we learn these linear coefficients from the device-charging history and estimate T_{cv} as

$$T_{\text{cv}} = e^{c \cdot log(C_{\text{cv}})} + d. \quad (13)$$

4. LABORATORY EXPERIMENTS

Real-life evaluation of `R-Aware`'s effectiveness in slowing down battery capacity fading is challenging owing to its dependency on user behavior. This is just as challenging as for Apple or Samsung to specify the operation time of their phones, in which case only the operation time under simplified conditions is provided, e.g., an up to 14-hour talk time on 3G for iPhone 6 without user interactions. In this section, we first detail our in-lab evaluation of the accuracy of `R-Aware` in predicting the charging process and its effectiveness in slowing down battery capacity fading. We then analyze its real-life effectiveness based on these experimental results as well as real-life user traces.

4.1 Collection of OCV–DoD Data

`R-Aware` needs the battery OCV–DoD table to plan the charging process. We use the battery tester as shown in Fig. 4 to charge the battery with 200mA current and sample the process at 1Hz, observing the relation between the battery terminal voltage and its DoD. We then perform resistance compensation on the thus-collected traces based on (2) to derive the OCV–DoD table. The small charging current is to reduce the $I \cdot r$ voltage and thus improve the accuracy of the derived OCD–DoD table. Likewise, we obtain the OCV–DoD curves in Fig. 10.

4.2 Accuracy in Charging Estimation

The accuracy in estimating the charging duration and charged capacity with a given profile is key to `R-Aware`. We collected 115 `R-Aware`-based charging traces with various charging profiles as summarized in Table 4. `R-Aware` takes these profiles as input to estimate the corresponding charging processes, which are then compared with the empirical traces to verify its estimation accuracy. Fig. 22 summarizes the estimation errors. The estimation errors in charged capacity are within 60mAh for 96% of the traces, with only 5 traces slightly off at 60.2mAh, 61.4mAh, 69.3mAh, 67.8mAh, and 61.0mAh. These errors correspond to a ratio of about $\frac{60}{2{,}600} \times 100\% = 2.3\%$ of the rated battery capacity. The error

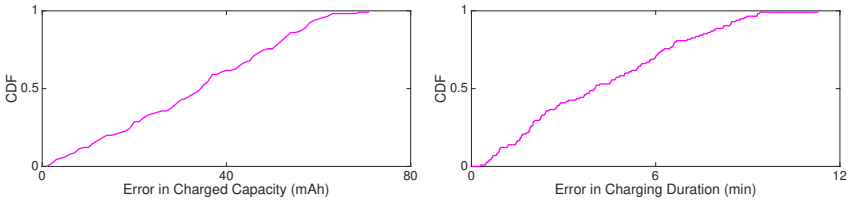

(a) Error in charged capacity **(b)** Error in charging duration

Figure 22: Accuracy of `R-Aware` in predicting the charging process.

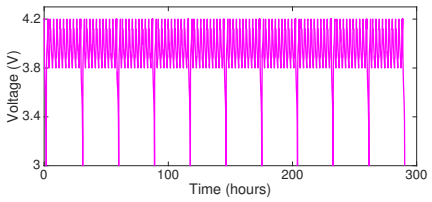

Figure 23: Voltage traces during one cycling measurements.

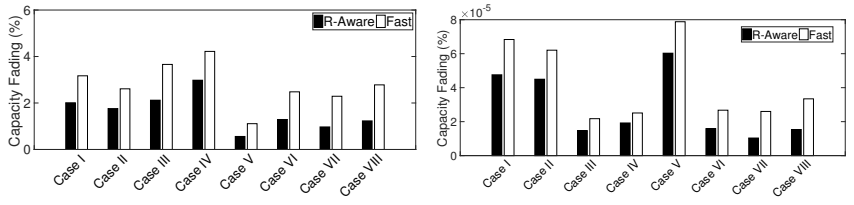

(a) Fading over the 100 cycles **(b)** Fading per delivered-capacity

Figure 24: `R-Aware` slows down battery capacity fading by up to 60%.

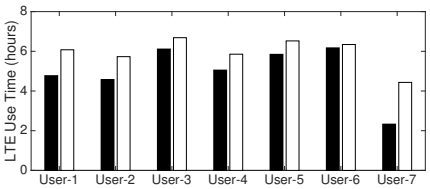

Figure 25: LTE time after 2-year usage

in estimating the charging duration is within 10 minutes for all traces with only an exception at 11.3 minute. This corresponds to an averaged ratio of 5.5% of their total charging durations.

4.3 Slowdown of Capacity Fading

We evaluate the effectiveness of `R-Aware` in slowing down the battery capacity fading. We conducted experiments with 8 batteries which are charged with both `R-Aware` and fast charging as summarized in Table 5. To study the capacity fading due to charge/discharge cycling, we discharged the charged batteries with a 500mA current until their OCVs decreased to the initial levels, and repeated the charge/discharge cycle 100 times. We fully charged and discharged the batteries every 10 such cycles to collect their total deliverable capacities. Each of these measurements lasts up to 16 days. Fig. 23 plots the voltage traces during one of these cycling tests as an illustration. Note that the fast charging process was terminated before batteries were fully charged due to the limited time available for charging. Fig. 24(a) shows the total capacity fading after these cycling measurements. The batteries fade 0.5–2% when charged with `R-Aware`, while those with fast charging fade 1–4.2%, showing a 43.9% slowdown of capacity fading on average. Averaging the capacity fading over the total capacity delivery during the measurements, Fig. 24(b) shows the batteries' fading rates per delivered-capacity. `R-Aware` shows the slowdown of capacity fading by 36.5% on average, and by up to 60% in certain extreme cases (e.g., Case-VII).

4.4 Trace-Driven Analysis

We also analyze the effectiveness of `iCharge` in real life based on the user-traces as shown in Fig. 3 (and Table 1) and the experimental results in Fig. 24 — what if `iCharge` is widely used in real life?

Fig. 24 shows an average capacity fading rate of 0.0161% and 0.0279% per cycle when the device is charged with `R-Aware` and incomplete fast charging, respectively. We further assume a 0.0161% fading rate when the device is charged completely with fast charging, which is reasonable because enough relaxation is applied to its battery as with `R-Aware`. We adopt the following linear model to estimate the fading rate in real life.

$$[0.0279\cdot(1-p)(1-q)+(0.0161\cdot(1-(1-p)(1-q))]\% \text{ / cycle}, \quad (14)$$

when the user chooses `R-Aware` to charge his device with probability p, and there is enough time to complete the charging with probability q if fast charging is selected.

Let's consider the following users' charging patterns.

- *Always-Fast:* Users always charge their devices with fast charging regardless of their available time, i.e., $p = 0$ in (14). This is the state-of-the-art mobile device charging.
- *Fast+R-Aware:* Under this mixed charging pattern, users charge their devices with fast charging if there is enough time for full charging; otherwise, they use `R-Aware` to keep their battery healthier, i.e., $q = 1$ in (14).

Nexus 5X is reported to have an initial 8-hour LTE use time [3], which gets shortened over usage due to capacity fading. Fig. 25 plots the estimated LTE time over a 2-year period for these 7 users when they charge the devices with the two patterns. The devices operate longer by up to 2.1 hours under the mixed charging pattern after 2 years when `iCharge` is equipped in them. Also, user behavior significantly affects device operation: higher chance of incomplete charging and higher frequency of charging make `iCharge` more effective in slowing down battery fading.

5. SMARTPHONE IMPLEMENTATION

We also implemented `R-Aware` on commodity Android phones to verify its feasibility and deployability.

5.1 Circuit Logic of R-Aware

Fig. 26 shows the circuit logic of `R-Aware` and compares it with the CCCV-based charging, such as fast charging. For CCCV, the current source outputs I_{cc} and the voltage source supplies $V_{\max}$. The switch selects CC-Chg or CV-Chg based

Table 6: Phone-based case-study results.

				Charging Time (min)			End-of-Charge SoC (%)		
Cases	**Device**	**Available Time**	**Initial SoC**	**Estimated**	**Ground Truth**	**Error**	**Estimated**	**Ground Truth**	**Error**
I	Nexus 5X	90min	29%	84.79	93.00	-8.21	62	68	-4
II	Nexus 5X	80min	50%	69.11	78.67	-9.56	76	78	-2
III	Nexus 5X	45min	6%	44.96	42.00	+2.96	14	15	-1
IV	Nexus 5X	45min	4%	42.32	39.00	+3.32	11	10	+1
V	Nexus 6P	60min	56%	59.72	63.00	-3.28	77	82	-5

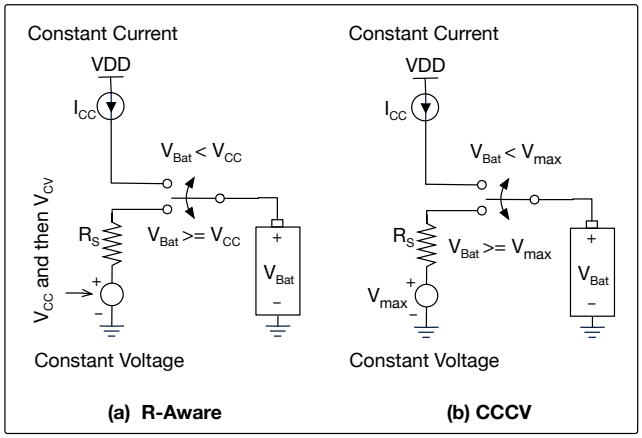

Figure 26: Circuit logic for `R-Aware` and CCCV: `R-Aware` does not require support of an additional circuit.

on real-time feedback of the battery voltage. On top of this CCCV implementation, `R-Aware` poses only one additional requirement for the voltage source to supply V_{cc} first and then V_{cv} — an evolution from one single voltage threshold to two voltage thresholds sequentially. This way, `R-Aware` does not require any additional circuit beyond existing CCCV implementation — all we need to do is to change the *soft* charging configuration.

5.2 Implementation Details

To implement `R-Aware` on mobile devices, we need (i) the ability to actively configure the charging profile, (ii) the OCV–DoD table of device battery, and (iii) the initial SoC of the device before charging.

Existing charger drivers on mobile devices support the active configuration of charging profile. In the case of Nexus 6P, for example, its battery charger driver defines the interfaces shown in Fig. 27 to configure the charging process. Specifically, the *qpnp_chg_ibatterm_set()* function allows for setting the terminating current I_{cutoff}, the maximum charging current can be set with *qpnp_chg_ibatmax_set()*, and V_{cc} and V_{cv} can be configured with the last two functions. Similar interfaces can be found in the kernels of other devices, such as Nexus 5X, Xperia Z, and Galaxy S6 Edge. The corresponding inputs to these interfaces can be accessed from the directory of /sys/class/power_supply/battery/. For example, V_{cc} and V_{cv} can be set by writing proper values to */sys/class/power_supply/battery/voltage_max*.

Similarly, writing a small current to file *current_max* facilitates to collect the OCV–DoD table of the device battery with high accuracy, similarly to the discussion in Sec. 4.1. Fig. 28 shows the thus-collected OCV–DoD curves of Nexus 5X and Nexus 6P phones with a maximum charging current of 300mA and 500mA, respectively.

Last but not the least, the real-time SoC of device batteries can be obtained using BatteryManager in Android, which also provides real-time battery voltage, allowing the logging of the charging process.

5.3 Validation of R-Aware's Implementation

We implemented `R-Aware` on Nexus 5X and 6P, and evaluated its performance via 5 case-studies, as summarized in Table 6. The errors of `R-Aware` in estimating the charging duration are within the range of $(-10, +4)$ minutes and those in the charged capacity are in the range of $(-5, +1)\%$. Fig. 29 shows the charging process in Case-I as an illustration, where $\times$ is the estimated charging results by `iCharge`. Another interesting observation is that there are two valleys in the voltage trace as highlighted. They occur because the battery temperature has risen to a pre-defined threshold of 45°C, forcing the charging current to be reduced (and thus the voltage to drop) for cooling. This, in turn, supports `R-Aware` that does not push for larger I_{cc}, as explained in Sec. 3.3.

6. USER STUDY

We have also conducted a user study to collect the detailed users' feedback on `iCharge`, such as whether users are willing to have their device battery equipped with additional interactive operations, and whether users want to use `R-Aware` for its extension of their device life despite its slower charging rate. The users study consists of two parts: a questionnaire-based survey and a conceptual app of `iCharge` users used in real-life.

6.1 User Survey

We surveyed 146 users to collect their charging behavior and opinions on `iCharge`. These participants are from 5 countries (US, Canada, Korea, Singapore, and China), aged from 15 to 40, and have various occupations such as government and commercial company employees, self-employers, school teachers, university faculties and students. The survey results corroborate the motivation of `iCharge`— i.e., slowing down the capacity fading of mobile device batteries is crucial — and demonstrate its attractiveness to users. Specifically,

- 80% of participants were aware that device charging affects battery fading;
- 89% of participants noticed the degradation of their device batteries over time;
- 70% of them regard it as crucial;
- 77% of them will use `iCharge` if available.

Moreover, with state-of-the-art charging solutions, 94% of the participants frequently prematurely terminated their

```
static int qpnp_chg_ibatterm_set(struct qpnp_chg_chip *chip,  int term_current){...};
static int qpnp_chg_ibatmax_set(struct qpnp_chg_chip *chip, int chg_current){...};
static int qpnp_chg_vddmax_and_trim_set(struct qpnp_chg_chip *chip, int voltage, in trim_mv){...};
static void qpnp_chg_adjust_vddmax(struct qpnp_chg_chip *chip, int vbat_mv){...};
```

Figure 27: Driver interfaces to configure the charging profile in Android kernel.

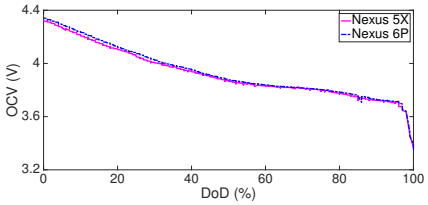

Figure 28: OCV–DoD curves collected from Nexus 5X and Nexus 6P.

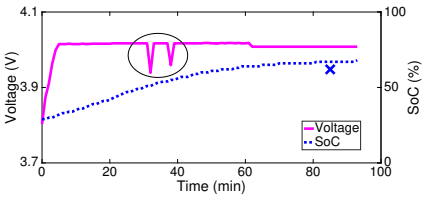

Figure 29: `R-Aware`-based charging process in Case-I on Nexus 5X.

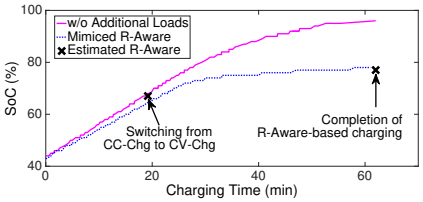

Figure 30: Mimicked `R-Aware`-based charging in the conceptual app of `iCharge`.

device charging, leading to incomplete CV-Chg; 52% of them charge their devices more than twice a day; less than 16% of them tried to charge only when they have enough time for fully charging the devices. These indicate a large room for improvement by `iCharge`.

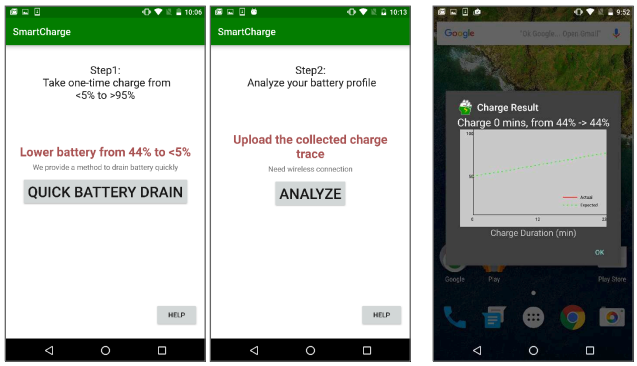

(a) Guide to finish initial training (b) Charge result

Figure 31: Conceptual app of `iCharge`. The user does one-time charging from below 5% to 95% or higher for the conceptual app to learn the battery. This charging process is displayed to the user after each charging.

6.2 Field Test with a Conceptual App

We further recruited 13 participants (6 females and 7 males) to use a conceptual Android app of `iCharge` in real-life. These participants are recruited from a user-study campaign posted online or at our university students center. None of them had prior knowledge of our research. After they agreed to participate in our user study, we sent them the conceptual app of `iCharge`, a short user manual, and a survey questionnaire regarding their opinion about `iCharge`. This user study was ruled by our university to be IRB non-regulated since it does not intrude user privacy nor records private information.

We refer this app to as *conceptual* because the system-level implementation of `R-Aware` introduced in Sec. 5 needs root permission of the device, which is not a feasible requirement for the user study participants. Instead, we "achieve" the same charging results as with `R-Aware`, but take a different approach.

Table 7: Controlling device power consumption to mimic `R-Aware`-based charging (Galaxy Note 4 as an example).

Level	Methodology	Load (mW)
1	WiFi scan every 500ms	508
2	WiFi scan every 250ms	635
3	Enable GPS Location Sensing	741
4	WiFi scan continuously	2,017
5	Math calculation every 500ms	2,824
6	Enable Microphone	2,853
7	Math calculation every 250ms	2,904
8	Enable inertial sensors	3,027
9	Math calculation continuously	5,554
10	Bluetooth scan	5,662

As explained in Fig. 18, the charger power is separated into two flows to charge the battery and power the device, respectively. Also, the charger's maximum output power is limited, e.g., 5V at 3A for Nexus 5X. This way, we can indirectly control the charging process by adjusting the power consumption of devices in the Android userspace, mimicking a `R-Aware`-based charging process. Specifically, the conceptual app uses 10 levels of cumulative power consumptions as summarized in Table 7 to regulate the charging process as if `R-Aware` were implemented. Our user-study verified these power consumption levels to be high enough to regulate the charging process. Fig. 30 shows one of thus-mimicked `R-Aware`-based charging process, which is slowed down to the estimated levels of `R-Aware` by adaptively adjusting the additional power consumptions.

A one-time training is required for the conceptual app to collect the basic information of device battery, such as its OCV–DoD table and resistance, by draining the battery to below 5% and then charging it to higher than 95%. Fig. 31 displays the user-interface to guide users to finish this initial training. This conceptual app records the user's input of available time and selection of a charging method, logs the charging process, and uploads the collected data to our server when a WiFi connection is available.

The conceptual app uses fast charging as default if no user input is collected from the UI within 5 minutes after the device plugged in a charger. The device will be continuously charged with I_{cutoff} if the user chooses `R-Aware` for charging but keeps the charger connected after the specified charging time elapsed, preserving the established equilibration. Also, users may disconnect the charger before their specified charging time elapses. Although `iCharge` cannot pre-

vent such cases, it would not cause additional fading when compared to the case where only fast charging is provided.

We have monitored the charging behavior of these 13 participants over an accumulated period of 28 weeks, collecting 319 charging cases of which

- 49% were day-time charging that lasts less than 2 hours, agreeing with the statistics shown in Fig. 3;
- 36% used `R-Aware` (up to 65% for certain specific users), showing users' willingness to care for their device batteries at the costs of slower charging rate and some user interactions;
- users completed their input on the available time and choose their preferred charging method within a medium of 8 seconds, validating the user-friendliness of `iCharge`; this interaction time decreases as users become more familiar with the UI.

7. EXTENSIONS AND IMPROVEMENTS

`iCharge` can be extended/improved in various ways some of which are discussed below.

7.1 iCharge as a Portable Charger

We have implemented `iCharge` on Android devices as a system component to control their charging process. An interactive portable charger would be another implementation choice. Actually, a few of the survey participants expressed their stronger preference to use `iCharge` if provided as a portable charger. To meet this need, we are now building a portable version of `iCharge` based on the programmable CCCV charger in [4].

7.2 iCharge for Electric Vehicles

Capacity fading exists in all battery-powered systems, including electric vehicles (EVs). In fact, `iCharge` is not only applicable to mobile devices, but also desperately needed for EVs for two reasons. First, the battery packs of EVs are expensive, e.g., replacing the 70kWh battery pack of Tesla Roadster costs as high as $\$29,000$ [7]. Slowdown of battery fading means reduced operating cost for users. It is also attractive to EV manufacturers as a slower fading rate reduces the battery pack size with the same warranty period, thus reducing the capital cost for users and increasing the competitiveness of products for manufacturers. Second, the available charging time would always be limited for certain types of EVs, e.g., taxis [9], causing pronounced capacity fading due to the early-termination of CV-Chg. This, on the other hand, offers more room for improvement with `iCharge`.

7.3 Enhancing iCharge with User Behaviors

`R-Aware`, the core of `iCharge`, needs users' available time as input to plan the charging, which is provided via a user-interactive interface. Yet, this incurs overhead to users (e.g., seconds of interaction time) and the users may not always follow their input (e.g., early disconnection of the charger before the specified time or keeping the connection after the charging time elapsed), both of which have been reflected in our user study introduced in Sec. 6.2. Another choice is to predict users' available charging time and needed power in real time by learning their usage behavior. This way, no additional user actions are required and the new charging paradigm offered by `iCharge` would be automatically triggered upon connecting the charger. The challenge, however, is to ensure high prediction accuracy so as not to degrade user experience. It is also possible to further improve the accuracy of `R-Aware` in predicting the charging process based on the user's charging history.

8. RELATED WORK

Existing efforts improve the limited operation time of mobile devices from two aspects: optimizing their energy consumption [15,17,21–23,30,33,37] and enhancing their energy-supply by charging faster [5, 10, 11].

Fast charging of batteries has been explored at different layers of abstraction, including algorithms [19,20,29,36], circuit topology [18], and specially-designed batteries [45]. For example, a variable frequency pulse charging system was proposed in [19] and a fuzzy-controlled charging design was presented in [29]. Boostcharging [36] advocates charging with large current by directly charging drained batteries in the CV mode. A grey predication-based charging algorithm was developed in [20]. A circuit topology for battery charging was proposed in [18], demonstrating the advantage of phase-locked loop. A unique type of Li-ion battery that can be charged in a few minutes was proposed in [45].

On the other hand, batteries get weakened over usage due to the loss of active materials [26, 27, 34, 38, 46], known as capacity fading. Efforts have been made to model the fading process [26,35], revealing that it is roughly linear [13,31,41, 46] and affected by various factors, such as current [32,35], temperature [26,43], DoD [35], etc.

In this paper, we discovered that CV-Chg slows down the capacity fading of batteries by allowing them to relax, corroborating the reported finding that relaxation after discharge helps improve the cycle life of batteries [40,41]. Also, we demonstrated that existing fast charging solutions may lead to incomplete CV-Chg due to their user-agnosia, thus accelerating the capacity fading of device batteries. To solve this problem, we proposed `iCharge` which customizes the device charging based on users' availability and need, and hence slows down the battery fading, opening a new charging paradigm for mobile devices.

9. CONCLUSIONS

We have and evaluated proposed a novel charging paradigm for mobile devices, called `iCharge`, that customizes the device charging based on users' real-time needs. At the core of `iCharge` is a relaxation-aware (`R-Aware`) charging algorithm that plans the device charging based on the user's available time, maximizing the charged capacity while ensuring the use of CV-Chg to relax the battery and thus slow down its capacity fading. `iCharge` also integrates `R-Aware` with fast charging via its interactions with users, allowing the users to choose a charging method based on their real-time needs. We have extensively evaluated `iCharge` via laboratory experiments, implementation on commodity phones, and user studies, all of which demonstrate the salient features of `iCharge`. Particularly, `iCharge` is shown to slow down the battery fading by 36% on average and up to 60% in certain extreme cases.

10. ACKNOWLEDGMENTS

The work reported in this paper was supported by NSF under Grant CNS-1446117.

11. REFERENCES

[1] Battery Monitoring Basics. https://training.ti.com/sites/default/files/BatteryMonitoringBasics.ppt.

[2] Lengthening the Life of Lithium-Ion Batteries. https://www.asme.org/engineering-topics/articles/energy/lengthening-life-of-lithiumion-batteries.

[3] Nexus 5X. https://store.google.com/product/nexus_5x.

[4] Programmable CCCV Charger. http://www.ti.com/tool/pmp8955.

[5] Quick Charge 3.0. http://www.droid-life.com/2015/09/14/qualcomm-quick-charge-3-0/.

[6] Survey shows battery life to be the single main gripe of today's mobile phone user. http://www.phonearena.com/news/Survey-shows-battery-life-to-be-the-single-main-gripe-of-todays-mobile-phone-user_id49818.

[7] Tesla Roadster battery pack replacement will cost $29,000. http://www.autoblog.com/2015/09/01/tesla-roadster-battery-pack-replacement/.

[8] The Care and Feeding of Lithium Polymer Batteries. http://forums.androidcentral.com/ambassador-guides-tips-how-s/500054-guide-care-feeding-lithium-polymer-batteries.html.

[9] The case for EV taxi. http://newyork.thecityatlas.org/lifestyle/the-case-for-the-electric-taxi/.

[10] TurboPower Charger. https://www.motorola.com/us/TurboPower/turbopower.html.

[11] VOOC Flash Charge. http://www.oppo.com/en/technology/vooc/.

[12] H. M. A. and T. Sasu. Understanding smartphone state of charge anomaly. In *HotPower'15*, 2015.

[13] L. Ahmadi, M. Fowler, S. B. Young, R. A. Fraser, B. Gaffney, and S. B. Walker. Energy efficiency of Li-ion battery packs re-used in stationary power applications. *Sustainable Energy Technologies and Assessments*, 8:9–17, 2014.

[14] A. Badam, R. Chandra, J. Dutra, A. Ferrese, S. Hodges, P. Hu, J. Meinershagen, T. Moscibroda, B. Priyantha, and E. Skiani. Software defined batteries. In *SOSP'15*, 2015.

[15] N. Balasubramanian, A. Balasubramanian, and A. Venkataramani. Energy consumption in mobile phones: a measurement study and implications for network applications. In *IMC'09*, 2009.

[16] Y. Barsukov and J. Qian. Battery power management for portable devices. *Artech House*, page 67, 2013.

[17] A. Carroll and G. Heiser. An analysis of power consumption in a smartphone. In *USENIXATC'10*, 2010.

[18] L.-R. Chen. PLL-based battery charge circuit topology. *Journal of Power Sources*, 51(6):1344–1346, 2004.

[19] L.-R. Chen. A design of an optimal battery pulse charge system by frequency-varied technique. *IEEE Transactions on Industrial Electronics*, 54(1):398–405, 2007.

[20] L.-R. Chen, R. C. Hsu, and C.-S. Liu. A design of a grey-predicted Li-ion battery charge system. *IEEE Transactions on Industrial Electronics*, 55(10):3692–3701, 2008.

[21] E. Cuervo, A. Balasubramanian, D. ki Cho, A. Wolman, S. Saroiu, R. Chandra, and P. Bahl. Maui: making smartphones last longer with code offload. In *MobiSys'10*, 2010.

[22] N. Ding, D. Wagner, X. Chen, A. Pathak, Y. C. Hu, and A. Rice. Characterizing and modeling the impact of wireless signal strength on smartphone battery drain. In *SIGMETRICS'13*, 2013.

[23] M. Dong, T. Lan, and L. Zhong. Rethink energy accounting with cooperative game theory. In *MobiCom'14*, 2014.

[24] D. Ferreira, A. K. Dey, and V. Kostakos. Understanding human-smartphone concerns: A study of battery life. In *Pervasive'11*, 2011.

[25] T. F. Fuller, M. Doyle, and J. Newman. Relaxation Phenomena in Lithium-Ion-Insertion Cells Thomas. *Journal of The Electrochemical Society*, 141(4):982–990, 1994.

[26] S. Grolleau, A. Delaille, H. Gualous, P. Gyan, R. Revel, J. Bernard, E. Redondo-Iglesias, and J. Peter. Calendar aging of commercial graphite/$LiFePO_4$ cell – Predicting capacity fade under time dependent storage conditions. *Journal of Power Sources*, 225:450–458, 2014.

[27] L. He, E. Kim, K. G. Shin, G. Meng, and T. He. Battery state-of-health estimation for mobile devices. In *ICCPS'17*, 2017.

[28] L. He, G. Meng, Y. Gu, C. Liu, J. Sun, T. Zhu, Y. Liu, and K. G. Shin. Battery-aware mobile data service. *IEEE Transactions on Mobile Computing*, 16(6):1544–1558, 2017.

[29] G.-C. Hsieh, L.-R. Chen, and K.-S. Huang. Fuzzy-controlled Li-ion battery charge system with active state-of-charge controller. *IEEE Transactions on Industrial Electronics*, 48(3):585–593, 2001.

[30] J. Huang, F. Qian, A. Gerber, Z. M. Mao, S. Sen, and O. Spatscheck. A close examination of performance and power characteristics of 4G LTE networks. In *MobiSys'12*, 2012.

[31] L. Lam and P. Bauer. Practical Capacity Fading Model for Li-Ion Battery Cells in Electric Vehicles. *IEEE Transactions on Power Electronics*, 28(12):5910–5918, 2013.

[32] B. Y. Liaw, E. P. Roth, R. G. Jungst, G. Nagasubramanian, H. L. Case, and D. H. Doughty. Correlation of Arrhenius behaviors in power and capacity fades with cell impedance and heat generation in cylindrical lithium-ion cells. *Journal of Power Sources*, 119(121):874–886, 2003.

[33] R. Mittal, A. Kansal, and R. Chandra. Empowering developers to estimate App energy consumption. In *MobiCom'12*, 2012.

[34] G. Ning, B. Haran, and B. N. Popov. Capacity fade study of lithium-ion batteries cycled at high discharge rates. *Journal of Power Sources*, 117:160–169, 2003.

[35] G. Ning and B. N. Popov. Cycle Life Modeling of Lithium-Ion Batteries. *Journal of The Electrochemical Society*, 151(10):A1584–A1591, 2004.

[36] P. Notten, J. O. het Veld, and J. van Beek. Boostcharging Li-ion batteries: A challenging new

charging concept. *Journal of Power Sources*, 145:89–94, 2005.

[37] A. Pathak, Y. C. Hu, and M. Zhang. Fine grained energy accounting on smartphones with Eprof. In *EuroSys'12*, 2012.

[38] M. B. Pinson and M. Z. Bazant. Theory of SEI Formation in Rechargeable Batteries: Capacity Fade, Accelerated Aging and Lifetime Prediction. *arXiv:1210.3672*, 2012.

[39] J. Qian. Li-ion battery-charger solutions for JEITA compliance. *Analog Applications Journal*, pages 8–11, 2010.

[40] M. Rashid and A. Gupta. Effect of relaxation periods over cycling performance of a Li-ion battery. *Journal of The Electrochemical Society*, 162(2):A3145–A3153, 2015.

[41] B. Saha and K. Goebel. Modeling Li-ion Battery Capacity Depletion in a Particle Filtering Framework. In *PHM'09*, 2009.

[42] A. Sanpei. Charging Method for Secondary Battery. US Patent, 5,237,259, 1993.

[43] H. Song, Z. Cao, X. Chen, H. Lu, M. Jia, Z. Zhang, Y. Lai, J. Li, and Y. Liu. Capacity fade of $LiFePO_4$/graphite cell at elevated temperature. *Journal of Solid State Electrochem*, 17:599–605, 2013.

[44] D. Wagner, A. Rice, and A. Beresford. Device analyzer: Understanding smartphone usage. In *MOBIQUITOUS'13*, 2013.

[45] K. Zaghib, M. Dontigny, A. Guerfi, P. Charest, I. Rodrigues, A. Mauger, and C. Julien. Safe and fast-charging Li-ion battery with long shelf life for power applications. *Journal of Power Sources*, 196:3949–3954, 2011.

[46] Y. Zhang and C.-Y. Wang. Cycle-Life Characterization of Automotive Lithium-Ion Batteries with $LiNiO_2$ Cathode. *Journal of The Electrochemical Society*, 156(7):A527–A535, 2009.